Published in final edited form as:
Bioorg Med Chem. 2012 July 15; 20(14): 4422–4429. doi:10.1016/j.bmc.2012.05.045.

Synthesis and Evaluation of *in Vitro* Bioactivity for Vesicular Acetylcholine Transporter Inhibitors Containing Two Carbonyl Groups

Zhude Tu[a,*], **Wei Wang**[a], **Jinquan Cui**[a], **Xiang Zhang**[a], **Xiaoxia Lu**[a], **Jinbin Xu**[a], and **Stanley M. Parsons**[b]

[a]Department of Radiology, Washington University, St. Louis, MO 63110.

[b]Department of Chemistry and Biochemistry and the Graduate Program in Biomolecular Science and Engineering, University of California, Santa Barbara, CA 93106.

Abstract

To identify selective high-affinity ligands for the vesicular acetylcholine transporter (VAChT), we have incorporated a carbonyl group into the structures of trozamicol and prezamicol scaffolds, and also converted the secondary amines of the piperidines of trozamicols and prezamicols into amides. Of 18 new racemic compounds, 4 compounds displayed high affinity for VAChT (K_i = 10 - 20 nM) and greater than 300-fold selectivity for VAChT over σ_1 and σ_2 receptors, namely (4-(4-fluorobenzoyl)-4'-hydroxy-[1,3'-bipiperidin]-1'-yl)(3-methylthiophen-2-yl)methanone oxalate (**9g**) ($K_{i\text{-VAChT}}$ = 11.4 nM, VAChT/σ_1 = 1063, VAChT/σ_2 = 370), (1'-benzoyl-4'-hydroxy-[1,3'-bipiperidin]-4-yl)(4-methoxyphenyl)methanone oxalate (**10c**) ($K_{i\text{-VAChT}}$ = 15.4 nM, VAChT/σ_1 = 374, VAChT/ σ_2 = 315), (4'-hydroxy-1'-(thiophene-2-carbonyl)-[1,3'-bipiperidin]-4-yl)(4-methoxyphenyl)methanone oxalate (**10e**) ($K_{i\text{-VAChT}}$ = 19.0 nM, VAChT/σ_1 = 1787, VAChT/ σ_2 = 335), and (4'-hydroxy-1'-(3-methylthiophene-2-carbonyl)-[1,3'-bipiperidin]-4-yl)(4-methoxyphenyl)methanone oxalate (**10g**) ($K_{i\text{-VAChT}}$ = 10.2 nM, VAChT/σ_1 = 1500, VAChT/ σ_2 = 2030). These 4 compounds can be radiosynthesized with C-11 or F-18 to validate their possibilities of serving as PET probes for quantifying the levels of VAChT *in vivo*.

Keywords

VAChT; σ receptor; Vesamciol; Parkinson Disease; CNS disorders

1. Introduction

The progressive loss of cognitive function is a characteristic feature of neurodegenerative disorders such as Alzheimer's disease, Down's syndrome, Parkinson disease, and schizophrenia. It is associated with the loss of cholinergic neurons and synapses in the brain.[1-6] Alteration of cholinergic function also has been implicated in drug addiction,

*Corresponding author. Tel.: +1-314-362-8487; fax: +1-314-362-8555; tuz@mir.wustl.edu.

Supplementary Material
Elemental analytical data of new analogues is available free of charge via internet.

especially to nicotine, ethanol, and neurostimulants such as cocaine, amphetamine, and opiates.[7, 8] Thus, the ability to quantitatively assess the status of cholinergic neurons in the brain will be very valuable for diagnosis of many neurological disorders and to monitor therapeutic efficacy. Positron emission tomography (PET) is a sensitive and non-invasive method to perform these tasks. When used with suitable radio-pharmaceuticals, PET imaging is able to provide biochemical and functional information on a living subject.

Vesicular acetylcholine transporter (VAChT), a 12 transmembrane domain protein discovered in the early 1980s, is a widely accepted biomarker for assessing the status of cholinergic neurons in the central nervous system.[9-11] It is located in the membrane of synaptic vesicles in the cholinergic presynaptic terminal and is responsible for transporting ACh and choline into the vesicles using a proton electrochemical gradient to drive transport.[12,13] Decreased VAChT expression strongly interferes with the loading of ACh into vesicles and further impairs the cognitive abilities of subjects.[13, 14]

Earlier studies have shown that VAChT tightly binds to the prototypical compound 2-(4-phenylpiperidino)cyclohexanol (vesamicol, **1**),[15-17] which blocks the ACh binding site in VAChT. Although vesamicol has nanomolar affinity for VAChT, it also has high affinity for σ_1 and σ_2 receptors, which are expressed throughout the brain.[18-20] As a result, the ability of vesamicol-like agents to accurately measure levels of VAChT in brain using PET is compromised. To solve this problem, investigators have tried to optimize the structure of vesamicol with the goals of retaining high VAChT affinity while reducing the σ receptor affinity, and improving the pharmacokinetics.[11, 19-22] The most significant improvement has been to identify benzovesamicol (**2**) analogues having high potency for VAChT binding. As an example, (-)-5-[^{123}I]iodobenzovesamicol ([^{123}I]IBVM, **3**) was used as a single photon emission computed tomography (SPECT) radio-tracer in patients with AD.[23] However, patients have to wait an undesirable 6 hr post-injection to attain equilibration before the SPECT scan.[21, 23] Until now, no clinically suitable PET tracer for quantifying VAChT in human brain has been reported. Recently, our group developed a new class of analogues, in which a carbonyl group is interposed between the phenyl and piperidine rings of the benzovesamicol structure. The in vitro data suggest that this new class of ligands can greatly reduce σ receptor binding and retain high VAChT binding.[24, 25] In particular, the two leading compounds (-)-trans-2-hydroxy-3-(4-(4-fluorobenzoyl)piperidino)-tetralin (**6**)[25] and 5-amino-3-[4-(4-fluorobenzoyl)piperidinyl]-2-hydroxy-1,2,3,4,-tetrahydro-naphthalene (**7**)[24] display high affinity and selectivity for VAChT versus σ receptors. More importantly, our initial in vivo validation suggested that (-)-[^{18}F]**6** is a very promising PET probe of VAChT.[25] In addition, (+)-benzoyltrozamicol (**(+)-4**) and (+)-4-fluorobenzyltrozamicol ((+)-[^{18}F]FBT, **5**)[26] have high VAChT binding affinities. Particularly, (+)-[^{18}F]FBT was reported as a very promising candidate to image VAChT in vivo,[27, 28] although it was later found that this compound is not suitable due to its high σ binding affinity and slow washout rate.[29]

To identify a PET radioligand possessing high potency and selectivity for VAChT in vivo, our group has continually explored the new class of analogues containing one or more carbonyl groups. In current study, the following strategies were employed: 1) retaining the carbonyl group between the phenyl group and piperidyl group in the 4-phenylpiperidyl moiety of the trozamicol scaffold; 2) converting the secondary amines in the trozamicol scaffold to tertiary amides using aromatic/heteroaromatic carboxylic acids; and 3) optimizing the substituents in the aromatic rings to improve the VAChT binding affinity of the new trozamicol scaffolds. In this manuscript, we report our work on the synthesis and in vitro bioactivity evaluation of these new analogues.

2. Results and Discussion

2.1. Chemistry

The target compounds were synthesized according to **Schemes 1-2**. The key trozamicol-like intermediates (1'-Benzoyl-4'-hydroxy-[1,3'-bipiperidin]-4-yl)(4-fluoro-phenyl)methanone (**8a**), and (1'-Benzoyl-4'-hydroxy-[1,3'-bipiperidin]-4-yl)(4-methoxy-phenyl)methanone (**8b**) as well as the key prezamicol-like intermediates(4-Fluorophenyl)(3'-hydroxy-[1,4'-bipiperidin]-4-yl)-methanone (**8c**), and (3'-Hydroxy-[1,4'-bipiperidin]-4-yl)(4-methoxyphenyl)-methanone (**8d**) were synthesized by following the procedure reported by our group.[30] We have previously reported the structural configuration of prezamicol by obtaining the x-ray crystal structure,[30] which allowed us to assign the structures of **8**. The target compounds **9a-g** and **10a-g** were prepared via trozamicol like intermediates **8a** or **8b** by acylating with various substituted benzoyl or substituted heteroaromatic carboxylic acids by using bis(2-oxo-3-oxazolidinyl)phosphinic chloride (BOPCl) coupling agent as shown in **Scheme 1**. Compounds **11a-d** were synthesized by following a similar synthetic procedure as for **9a-g** or **10a-g**, except the prezamicol-like intermediates **8c** or **8d** replacing trezamicol-like **8a** or **8b** as shown in **Scheme 2**. All the products were dissolved in acetone or acetone/ethanol solvent and treated with oxalic acid to convert into the oxalate salts of **9a-g, 10a-g** and **11a-d** for determining binding affinities.

2.2. Biological binding studies

Competitive inhibition of the binding of different radioligands under highly selective conditions was performed to estimate the σ_1,σ_2, and VAChT affinities (K_i, nM) of **9a-g, 10a-g** and **11ad**.[24, 25, 30] The details are given in Section 4.5. Apparent dissociation constants for *in vitro* binding of the novel compounds are given in **Table 1**.

Compounds **9g**, **10c**, **10e** and **10g** displayed high affinity for VAChT (K_i < 20 nM) and much higher selectivity for VAChT relative to σ_1 and σ_2 receptors (at least > 300 fold). Moreover, a few interesting structure-activity trends were identified. Firstly, the strategy of converting the secondary amine of trozamicol-like structures (**8a** and **8b**) to tertiary amides (**9a-g** and **10a-g**) successfully reduced the binding affinities for σ receptors; the new amide analogues displayed very low affinity for σ_1 (K_i > 1300 nM) and σ_2 (K_i > 2500 nM) receptors with the exception of compound **9b** (K_i = 661 nM for σ_1). We previously reported that when the secondary amine of trozamicol is converted to a tertiary amine by benzylation, binding affinity toward σ_1 receptor is high.[30] Secondly, thiophene derivatives of the new amide analogues **9g** (K_i = 11.4 ± 3.67 nM) and **10g** (K_i = 10.2 ± 0.76 nM) have higher affinities for VAChT than vesamicol does. More importantly, both new compounds have very low σ affinities. For **9g**, K_i = 12100 ± 2400 nM for σ_1 and 4220 ± 200 nM for σ_2. For **10g**, K_i = 15300 ± 2870 nM for σ_1 and 20700 ± 2670 nM for σ_2. The selectivity of VAChT vs. σ receptors for **9g** was greater than 370 fold and that for **10g** was greater than 1500-fold, both of which are much higher than for vesamicol. As VAChT binds to the ligands enantioselectively,[31] it is expected that one of the corresponding enantiomers of the new potent compounds **9g** and **10g** will have much higher binding affinity for VAChT than the racemic mixtures do.

Furthermore, in the para-position to the carbonyl group of the 4-fluorobenzoylpiperidinyl fragment, compounds **9g** and **10g** contain either a fluorine atom or a methoxy group, respectively, which is suitable for replacement with [^{18}F] or [^{11}C]CH_3 that can be used in PET imaging studies. Compound [^{18}F]**9g** can be made easily by the displacement of the nitro group of a corresponding precursor with K[^{18}F]/fluoride[25], and [^{11}C]**10g** can be made easily by reacting corresponding desmethyl phenol substrate with [^{11}C]CH_3I in the presence of base. The Log P values of **9g** and **10g** are 2.53 and 2.51 respectively, suggesting that **9g**

and **10g** have suitable lipophilicity for crossing the brain blood barrier (BBB) into the brain. If further in vitro studies of both **9g** and **10g** confirm they have high affinity and selectivity for VAChT, the potent isomer of [^{18}F]**9g** or [^{11}C]**10g** is worth exploring further in vivo.

With the exception of **9g** and **10g**, compounds in the **10** series that contain an electron-rich methoxy substitution para to the carbonyl of the ketone favored VAChT binding over compounds in the **9** series that contain an electron-withdraw fluoro substitution para to the carbonyl of the ketone. VAChT binding affinity was increased 37-fold from **9a** (8700 ± 1620 nM) to **10a (**233 ± 37 nM), 4.3-fold from **9b** (13000 ± 1900 nM) to **10b (**3020 ± 640 nM), 4-fold from **9c** (62.7 ± 14.3 nM) to **10c (**15.4 ± 0.94 nM), 7.2-fold from **9d** (807 ± 139 nM) to **10d** (112 ± 13 nM), 6.4-fold from **9e** (123 ± 14 nM) to **10e** (19.0 ± 2.12 nM), and 8.4-fold from **9f** (1190 ± 137 nM) to **10f (**142 ± 16.4 nM). This suggests that the electron-rich methoxy substitution is important for VAChT binding.

In ligands **9a**, **9b** and **9c**, where a fluorine atom is para to the ketone carbonyl, both fluoro substituted **9a** (K_i = 8700 ± 1620 nM) and methoxy substituted **9b** (K_i = 13000 ± 1900 nM) para to the amide carbonyl displayed dramatic reductions in binding affinity compared to that of unsubstituted benzamide **9c** (K_i = 62.7 ± 14.3 nM). The binding affinities of compounds **9a** and **9b** were reduced approximately 139- and 207-fold compared to **9c**. A similar trend was observed for compounds **10a, 10b** and **10c**, for which the decrease in binding affinities were 15-fold and 196-fold, respectively, relative to compound **10c**. Comparison of compounds **9d** vs **9c**, and of **10d** vs **10c**, shows that the 3-pyridyl amides exhibit decreases in affinity for VAChT compared to the benzamides.

Compounds **9e** and **10e** which contain the thiophene-2-carbonyl group showed decreased affinity for VAChT compared to **9c** and **10c** which contain the benzoyl group. The reduction in affinity was minor; 2-fold from **9c** (K_i = 62.7 ± 14.3 nM) to **9e** (K_i = 123 ± 14.9 nM) and 1.2-fold from **10c** (K_i = 15.4 ± 0.94 nM) to **10e** (K_i = 19.0 ± 2.12 nM). When a methyl group was introduced at the 3- or 5-position in thiophene-2-carbonyl containing compounds, **9f** and **9g** were obtained. The minor structural differences cause remarkable changes in the affinities. Compound **9e** has a modest to low VAChT binding affinity (K_i = 123 ± 14.9 nM), and compound **9f** has very low VAChT binding affinity (K_i = 1190 ± 137 nM). A similar trend was observed for compounds **10e** and **10f**, as the affinity reduced 7-fold from **10e** (K_i = 19.0 ± 2.12 nM) to **10f** (K_i = 142 ± 16.4 nM). However, when the position of the methyl group was changed from position 5 to position 3 (**9g** to **9f**), the affinity increased by 104-fold from K_i = 1190 ± 137 nM for **9f** to K_i = 11.4 ± 3.67 nM for **9g.** The VAChT binding affinity of **9g** was approximately 6-fold higher than the affinities of **9c** and vesamicol (K_i = 15.2 ± 1.05 nM). Similar results were observed for compounds **10f** (K_i = 142 ± 16.4 nM) and **10g** (10.2 ± 0.76 nM). This result demonstrates that the position of the substituent on the thiophene in this new class of ligands is very critical to VAChT binding. Substitution at various positions may have different steric effects, which result in dramatic change in the affinity of these ligands.

This observation provides important information for further structure-activity relationship studies. To test the impact of thiophene and methyl substituted thiophenes in the prezamicol-like scaffold, compounds **11a-d** were synthesized, and their binding affinities for VAChT were determined. For **11a**, **11b**, **11c** and **11d**, the K_i values are 1300 ± 193 nM, 2020 ± 482 nM, 206 ± 21.8 nM and 1350 ± 433 nM, respectively. This result shows that thiophene and substituted thiophenes in the prezamcol-like scaffold (**11a-d**) show lower binding affinities. The observation is consistent to the reported result that prezamicol analogues are less potent toward VAChT.[30]

In summary, our approaches to optimizing the structure of trozamicol analogue, fluorobenzoyltrozamicol (FBT) include: (1) introducing a carbonyl group between the aromatic and piperi-dine rings; (2) replacing the substituted benzyl group of tertiary amines with a substituted benzoyl group to make tertiary amides. These approaches not only retain high VAChT affinity, but also greatly decrease the σ binding affinities of trozamicol analogues and increase selectivity for VAChT vs. σ receptors. Electronic effects of substitution at the position para to the ketone carbonyl in trozamicol-like analogues have a predominant effect; ligands with electron-rich methoxy substitution (**10**) display higher potencies toward VAChT compared to ligands with fluoro substitution (**9**). When the amide part of trozamicol-like ligands is substituted with 3-methyl-thiophene-2-amide, two new racemic ligands **9g** and **10g** were obtained that display high affinity (K_i value ~10 nM) and selectivity for VAChT. In current work, the binding affinities were measured only for new synthesized racemic compounds. Racemates having high potency for VAChT and high selectivity for VAChT versus σ receptors will be further resolved in future to obtain corresponding enantiomers. Due to the VAChT stereoselective binding property, it is expected that the more potent enantiomers will have higher potency and higher selectivity than that of the corresponding racemates have. Nevertheless, these results reported here, provide important new information for structure-activity analysis, which could lead to identification of suitable PET tracers for imaging VAChT in vivo.

3. Conclusion

In this study, we reported our exploration on the development of new VAChT analogues based on a hybrid structure of fluorobenzyltrozamicol **5** and **6**. Our structural modifications led us to four potent ligands, namely **9g** (K_i = 11.4 nM), **10c** (K_i = 15.4 nM), **10e** (K_i = 19.0 nM), and **10g** (K_i = 10.2 nM) having similar or higher affinity for VAChT compared to that of vesamicol. However, the selectivity for VAChT vs. σ receptors is much higher than for prior VAChT ligands. Particularly, two of the most potent ligands, **9g** and **10g** displayed high selectivity over σ receptors. For **9g**, the selectivity reached 1063-fold, and 370-fold of VAChT versus σ_1 and σ_2 receptor; for **10g,** it reached 1500-fold, 2030-fold of VAChT versus σ_1 and σ_2 respectively.

4. Experimental

4.1. General

All reagents and chemicals were purchased from commercial suppliers and used without further purification unless otherwise stated. All anhydrous reactions were carried out in oven-dried glassware under an inert nitrogen atmosphere unless otherwise stated. Flash column chromatography was conducted on silica gel 60A “40 Micron Flash” [32-63μm] (Scientific absorbents, INC); the mobile phase used is reported in the experimental procedure for each compound. Melting points were determined using the MEL-TEMP 3.0 apparatus and left uncorrected. ^{1}HNMR spectra were recorded at 400 MHz on a Varian Mercury-VX spectrometer with $CDCl_3$ as solvent and tetramethylsilane (TMS) as the internal standard unless otherwise stated. All chemical shift values are reported in parts per million (ppm) (δ). Peak multiplicities are singlet, s; doublet, d; triplet t; multiplet, m; broad, br. Elemental analyses (C, H, N) were determined by Atlantic Microlab, Inc. Elemental analysis was used to determine the purity of the target compounds that were assessed in vitro. All the compounds reported in the manuscript have a purity of ≥95%.

4.2. Procedure C. General method of preparing 9a-g,10a-g and 11a-b by aroylation of piperidines 8a-d and conversion to the corresponding oxalates

4.2.1. (4'-Hydroxy-[1,3'-bipiperidine]-1',4-diyl)bis(4-fluorophenyl)methanone oxalate (9a)—In a solution of **8a** (56 mg, 0.183 mmol), BOPCl (100 mg, 0.40 mmol), triethylamine (1 mL) in methylene chloride (30 mL), 4-fluorobenzoic acid (40 mg, 0.285 mmol) was added. The reaction mixture was stirred overnight at room temperature. The reaction mixture was washed with saturated aqueous Na_2CO_3 (20 mL × 5) and brine solution (20 mL). The organic phase was dried over Na_2SO_4 and concentrated under vacuum. The crude product was purified by silica gel column chromatography using ethyl acetate followed by ethyl acetate/triethylamine (98/2, v/v) to afford **9a** as a colorless oil (76 mg, 97%). ^{1}H NMR (400 MHz, $CDCl_3$) δ 7.96 (t, *J* = 6.9 Hz, 2H), 7.50 – 7.36 (m, 2H), 7.13 (dt, *J* = 12.2, 8.5 Hz, 4H), 4.87 (br s, 1H), 3.98 – 3.46 (m, 3H), 3.35 – 3.16 (m, 1H), 3.16 – 2.58 (m, 5H), 2.52 – 2.27 (m, 2H), 2.22 – 2.00 (m, 1H), 2.01 – 1.67 (m, 4H), 1.56 – 1.34 (m, 1H). ^{13}C NMR (101 MHz, $CDCl_3$) δ 200.6, 169.7, 164.7, 164.6, 132.2, 131.7, 130.9, 129.2, 116.0, 115.7, 67.8, 67.4, 52.3, 45.2, 43.6, 32.8, 29.5, 29.1. The free base was converted to the oxalate by dissolving in acetone and mixing with 1 equivalent of oxalic acid to afford the corresponding oxalate salt as white solid. mp: 151 °C (decomposed). Anal. ($C_{24}H_{26}F_2N_2O_3$ •$H_2C_2O_4$•0.5H_2O) C, H, N.

4.2.2. (4-(4-Fluorobenzoyl)-4'-hydroxy-[1,3'-bipiperidin]-1'-yl)(4-methoxyphenyl)methanone oxalate (9b)—Free base **9b** (105 mg, 55%) was obtained as a light yellow solid.^{1}H NMR (400 MHz, $CDCl_3$) δ 7.96 (dd, *J* = 8.6, 5.4 Hz, 2H), 7.38 (d, *J* = 8.7 Hz, 2H), 7.14 (t, *J* = 8.6 Hz, 2H), 6.93 (d, *J* = 8.7 Hz, 2H), 4.99 – 4.58 (br s, 1H), 3.84 (s, 3H), 3.74 – 3.51 (m, 2H), 3.29 – 3.14 (m, 1H), 3.14 – 3.03 (m, 1H), 3.01 – 2.59 (m, 4H), 2.51 – 2.22 (m, 2H), 2.17 – 2.05 (m, 1H), 1.97 – 1.81 (m, 3H), 1.81 – 1.67 (m, 1H), 1.59 – 1.43 (m, 1H). ^{13}C NMR (101 MHz, $CDCl_3$) δ 200.6, 170.5, 166.9, 160.8, 132.2, 130.8, 128.8, 127.7, 115.9, 113.7, 68.0, 67.4, 55.3, 52.1, 45.1, 43.5, 32.7, 29.4, 29.0. The free base was treated with oxalic acid to afford the corresponding oxalate salt as white solid. mp: 217 °C (decompose). Anal. ($C_{25}H_{29}FN_2O_4$•$H_2C_2O_4$) C, H, N.

4.2.3. (1'-Benzoyl-4'-hydroxy-[1,3'-bipiperidin]-4-yl)(4-fluoro-phenyl)methanone oxalate (9c)—Free base **9c** (0.20 g, 65%) was obtained as a pale solid .^{1}H NMR (400 MHz, $CDCl_3$) δ 8.06 – 7.77 (br s, 2H), 7.49 – 7.29 (m, 5H), 7.13 (t, *J* = 8.4 Hz, 2H), 5.01 – 4.59 (m, 1H), 3.97 – 3.58 (m, 3H), 3.33 – 3.17 (m, 1H), 3.16 – 2.57 (m, 5H), 2.54 – 2.30 (m, 2H), 2.11 – 1.98 (m, 1H), 1.98 – 1.65 (m, 4H), 1.62 – 1.35 (m, 1H). ^{13}C NMR (101 MHz, $CDCl_3$) δ 200.6, 170.6, 166.9, 163.4, 130.9, 129.8, 128.5, 126.7, 115.9, 113.8, 67.6, 67.4, 52.3, 45.2, 43.5, 32.9, 29.4, 29.0. The free base was converted to the oxalate salt as white solid. mp: 193 °C (decomposed). Anal. ($C_{24}H_{27}FN_2O_3$•$H_2C_2O_4$• H_2O) C, H, N.

4.2.4. (4-(4-Fluorobenzoyl)-4'-hydroxy-[1,3'-bipiperidin]-1'-yl)(pyridin-3-yl)methanone oxalate (9d)—Free base **9d** (33 mg, 81%) was obtained as a grease oil. ^{1}H NMR (400 MHz, $CDCl_3$) δ 8.75 – 8.60 (m, 2H), 8.03 – 7.84 (m, 2H), 7.76 (d, *J* = 7.7 Hz, 1H), 7.43 – 7.31 (m, 1H), 7.14 (t, *J* = 8.5 Hz, 2H), 4.99 – 4.67 (m, 1H), 3.91 – 3.49 (m, 3H), 3.32 – 3.18 (m, 1H), 3.17 – 2.61 (m, 5H), 2.51 – 2.33 (m, 2H), 2.15 – 2.03 (m, 1H), 1.99 – 1.68 (m, 4H), 1.54 – 1.39 (m, 1H). ^{13}C NMR (101 MHz, $CDCl_3$) δ 200.6, 167.9, 164.5, 151.0, 147.8, 134.9, 132.3, 131.6, 130.8, 123.6, 115.8, 67.5, 67.3, 45.3, 43.6, 39.7, 33.0, 29.5, 29.1. The free base was treated with oxalic acid to afford the corresponding oxalate salt as white solid. mp: 139 °C (decomposed). Anal. ($C_{23}H_{26}FN_3O_3$•$H_2C_2O_4$• H_2O) C, H, N.

4.2.5. (4-(4-Fluorobenzoyl)-4'-hydroxy-[1,3'-bipiperidin]-1'-yl)-(thiophen-2-yl)methanone oxalate (9e)—Free base **9e** (26 mg, 64%) was obtained as a grease oil. ^{1}H

NMR (400 MHz, $CDCl_3$)δ 7.96 (dd, *J* = 8.7, 5.4 Hz, 2H), 7.46 (d, *J* = 5.8 Hz, 1H), 7.30 (d, *J* = 3.6 Hz, 1H), 7.14 (t, *J* = 8.6 Hz, 2H), 7.10 – 7.01 (m, 1H), 4.83 – 4.58 (br s, 1H), 4.50 – 4.27 (br s, 1H), 3.71 (td, *J* = 10.3, 4.8 Hz, 1H), 3.65 – 3.50 (br s, 1H), 3.29 – 3.17 (m, 1H), 3.14 – 3.04 (m, 1H), 3.04 – 2.65 (m, 4H), 2.52 – 2.29 (m, 2H), 2.21 – 2.08 (m, 1H), 1.97 – 1.68 (m, 4H), 1.61 – 1.47 (m, 1H). ^{13}C NMR (101 MHz, $CDCl_3$) δ 200.6, 166.9, 163.8, 136.8, 132.3, 130.9, 130.8, 128.8, 126.7, 115.7, 67.9, 67.4, 52.2, 45.2, 43.6, 32.7, 29.5, 29.1. The free base was treated with oxalic acid to afford the corresponding oxalate salt as white solid. mp: 160 °C (decomposed). Anal. ($C_{22}H_{25}FN_2O_3S•H_2C_2O_4•H_2O$) C, H, N.

4.2.6. (4-(4-Fluorobenzoyl)-4'-hydroxy-[1,3'-bipiperidin]-1'-yl)(5-methylthiophen-2-yl)methanone oxalate (9f)—Free base **9f** (33 mg, 77%) was obtained as a greasy oil. ^{1}H NMR (400 MHz, $CDCl_3$) δ 8.00 – 7.91 (m, 2H), 7.18 – 7.08 (m, 3H), 6.75 – 6.67 (m, 1H), 4.77 – 4.60 (m, 1H), 4.51 – 4.35 (m, 1H), 3.70 (td, *J* = 10.3, 4.7 Hz, 1H), 3.62 – 3.52 (br s, 1H), 3.30 – 3.17 (m, 1H), 3.13 – 3.04 (m, 1H), 3.02 – 2.82 (m, 3H), 2.80 – 2.68 (m, 1H), 2.51 (s, 3H), 2.48 – 2.31 (m, 2H), 2.20 – 2.10 (m, 1H), 1.97 – 1.67 (m, 4H), 1.61 – 1.45 (m, 1H). ^{13}C NMR (101 MHz, $CDCl_3$) δ 200.6, 167.0, 169.8, 144.0, 134.4, 132.3, 130.9, 129.3, 125.1, 115.7, 67.9, 67.5, 52.2, 45.2, 43.6, 32.7, 29.5, 29.2, 15.3. The free base was treated with oxalic acid to afford the corresponding oxalate salt as white solid. mp: 140 °C (decomposed). Anal. ($C_{23}H_{27}FN_2O_3S•H_2C_2O_4$) C, H, N.

4.2.7. (4-(4-Fluorobenzoyl)-4'-hydroxy-[1,3'-bipiperidin]-1'-yl)(3-methylthiophen-2-yl)methanone oxalate (9g)—Free base **9g** (53 mg, 76%) was obtained as a colorless oil. ^{1}H NMR (400 MHz, $CDCl_3$) δ 8.00 – 7.90 (m, 2H), 7.29 (d, *J* = 5.0 Hz, 1H), 7.14 (t, *J* = 8.6 Hz, 2H), 6.86 (d, *J* = 5.0 Hz, 1H), 4.69 – 4.38 (br s, 1H), 4.23 – 3.99 (br s, 1H), 3.75 – 3.52 (m, 2H), 3.28 – 3.16 (m, 1H), 3.13 – 3.00 (m, 1H), 2.98 – 2.68 (m, 4H), 2.51 – 2.30 (m, 2H), 2.28 (s, 3H), 2.16 – 2.07 (m, 1H), 1.96 – 1.66 (m, 4H), 1.60 – 1.42 (m, 1H). ^{13}C NMR (101 MHz, $CDCl_3$) δ 200.6, 166.9, 164.8, 137.5, 132.2, 130.7, 129.9, 129.7, 125.8, 115.9, 67.9, 67.3, 52.1, 45.2, 43.5, 32.6, 29.4, 29.1, 14.6. The free base was treated with oxalic acid to afford the corresponding oxalate salt as white solid. mp: 146 °C (decomposed). Anal. ($C_{23}H_{27}FN_2O_3S•H_2C_2O_4•0.25H_2O$) C, H, N.

4.2.8. (1'-(4-Fluorobenzoyl)-4'-hydroxy-[1,3'-bipiperidin]-4-yl)(4-methoxyphenyl)methanone oxalate (10a)—Free base **10a** (90 mg, 82%) was obtained as a white solid. ^{1}H NMR (400 MHz, $CDCl_3$) δ 7.91 (d, *J* = 8.4 Hz, 2H), 7.45 – 7.35 (m, 2H), 7.11 (t, *J* = 8.5 Hz, 2H), 6.94 (d, *J* = 8.5 Hz, 2H), 4.98 – 4.72 (br s, 1H), 3.87 (s, 3H), 3.76 – 3.50 (m, 3H), 3.32 – 3.15 (m, 1H), 3.11 – 2.58 (m, 5H), 2.49 – 2.29 (m, 2H), 2.18 – 1.99 (m, 1H), 1.96 – 1.61 (m, 4H), 1.57 – 1.36 (m, 1H). ^{13}C NMR (101 MHz, $CDCl_3$) δ 200.7, 169.7, 164.7, 163.5, 131.7, 130.5, 129.0, 128.8, 115.5, 113.8, 67.7, 67.4, 55.5, 52.4, 45.2, 43.3, 32.8, 29.7, 29.2. The free base was treated with oxalic acid to afford the corresponding oxalate salt as white solid. mp: 192 °C (decomposed). Anal. ($C_{25}H_{29}FN_2O_4•H_2C_2O_4•1.5H_2O$) C, H, N.

4.2.9. (1'-(4-Methoxybenzoyl)-4'-hydroxy-[1,3'-bipiperidine]-4-yl)(4-methoxyphenyl)methanone oxalate (10b)—Free base **10b** (234 mg, 62%) was obtained as a light yellow solid.^{1}H NMR (400 MHz, $CDCl_3$) δ 7.89 (d, *J* = 8.5 Hz, 2H), 7.35 (d, *J* = 8.6 Hz, 2H), 6.97 – 6.82 (m, 4H), 4.95 – 4.60 (br s, 1H), 3.84 (s, 3H), 3.82 (s, 3H), 3.71 – 3.51 (m, 2H), 3.27 – 3.12 (m, 1H), 3.12 – 2.98 (m, 1H), 2.98 – 2.55 (m, 4H), 2.47 – 2.19 (m, 2H), 2.16 – 2.03 (m, 1H), 1.91 – 1.64 (m, 4H), 1.57 – 1.39 (m, 1H). ^{13}C NMR (101 MHz, $CDCl_3$) δ 200.7, 170.5, 163.4, 160.7, 130.4, 128.8, 128.7, 127.7, 113.8, 113.7, 67.8, 67.4, 55.4, 55.3, 52.3, 45.2, 43.2, 32.7, 29.6, 29.2. The free base was treated with oxalic acid to afford the corresponding oxalate salt as white solid. mp: 164 °C (decomposed). Anal. ($C_{26}H_{32}N_2O_5.C_2H_2O_4$) C, H, N.

4.2.10. (1'-Benzoyl-4'-hydroxy-[1,3'-bipiperidin]-4-yl)(4-methoxy-phenyl)methanone oxalate (10c)—Free base **10c** (0.134 g, 74%) was obtained as a white solid. ^{1}H NMR (400 MHz, $CDCl_3$) δ 8.01 – 7.78 (m, 2H), 7.48 – 7.31 (m, 5H), 6.94 (d, *J* = 8.0 Hz, 2H), 4.97-4.60 (m, 1H), 3.84 (s, 3H), 3.81 – 3.56 (m, 3H), 3.35 – 2.60 (m, 6H), 2.56 – 2.31 (m, 2H), 2.30 – 2.13 (m, 1H), 2.00 – 1.70 (m, 4H), 1.63 – 1.40 (m, 1H). ^{13}C NMR (101 MHz, $CDCl_3$) δ 200.8, 170.7, 163.5, 135.8, 130.5, 130.0, 128.8, 128.6, 126.8, 113.9, 67.8, 67.4, 55.5, 52.2, 45.2, 43.2, 32.9, 29.7, 29.3. The free base was treated with oxalic acid to afford the corresponding oxa-late salt as white solid. mp: 180 °C (decomposed). Anal. ($C_{25}H_{30}N_2O_4 \cdot H_2C_2O_4 \cdot H_2O$) C, H, N.

4.2.11. (4'-Hydroxy-1'-nicotinoyl-[1,3'-bipiperidin]-4-yl)(4-methoxy-phenyl)methanone oxalate (10d)—Free base **10d** (36 mg, 90%) was obtained as a colorless grease. ^{1}H NMR (400 MHz, $CDCl_3$) δ 8.72 – 8.64 (m, 2H), 7.96 – 7.85 (m, 2H), 7.76 (d, *J* = 7.7 Hz, 1H), 7.38 (t, *J* = 6.3 Hz, 1H), 6.94 (d, *J* = 8.4 Hz, 2H), 4.99 – 4.68 (m, 1H), 3.87 (s, 3H), 3.79 – 3.59 (m, 2H), 3.34 – 3.19 (m, 1H), 3.12 – 2.62 (m, 5H), 2.51 – 2.33 (m, 2H), 2.28 – 2.05 (m, 1H), 1.98 – 1.71 (m, 4H), 1.49 (s, 1H). ^{13}C NMR (101 MHz, $CDCl_3$) δ 200.7, 168.0, 163.5, 151.0, 147.8, 134.8, 131.6, 130.5, 128.8, 123.6, 113.9, 67.6, 67.3, 55.5, 52.5, 45.3, 43.3, 33.0, 29.7, 29.2. The free base was treated with oxalic acid to afford the corresponding oxalate salt as white solid. mp: 148 °C (decomposed). Anal. ($C_{24}H_{29}N_3O_4 \cdot H_2C_2O_4 \cdot 1.5H_2O$) C, H, N.

4.2.12. (4'-Hydroxy-1'-(thiophene-2-carbonyl)-[1,3'-bipiperidin]-4-yl)(4-methoxyphenyl)methanone oxalate (10e)—Free base **10e** (22 mg, 55%) was obtained as a colorless oil. ^{1}H NMR (400 MHz, $CDCl_3$) δ 7.92 (d, *J* = 8.9 Hz, 2H), 7.46 (dd, *J* = 5.1, 1.2 Hz, 1H), 7.31 (dd, *J* = 3.7, 1.3 Hz, 1H), 7.06 (dd, *J* = 5.0, 3.6 Hz, 1H), 6.94 (d, *J* = 8.9 Hz, 2H), 4.78 – 4.54 (br s, 1H), 4.50 – 4.30 (br s, 1H), 3.86 (s, 3H), 3.77 – 3.59 (m, 2H), 3.30 – 3.17 (m, 1H), 3.15 – 3.03 (m, 1H), 3.03 – 2.71 (m, 4H), 2.52 – 2.31 (m, 2H), 2.22 – 2.09 (m, 1H), 1.93 – 1.66 (m, 4H), 1.61 – 1.46 (m, 1H). ^{13}C NMR (101 MHz, $CDCl_3$) δ 200.6, 163.5, 163.2, 136.6, 130.3, 128.6, 128.5, 128.4, 126.6, 113.6, 67.7, 67.2, 55.3, 52.0, 45.1, 43.0, 32.5, 29.4, 29.1. The free base was treated with oxalic acid to afford the corresponding oxalate salt as white solid. mp: 137 °C (decomposed). Anal. ($C_{23}H_{28}N_2O_4S \cdot H_2C_2O_4 \cdot 0.5H_2O$) C, H, N.

4.2.13. (4'-Hydroxy-1'-(5-methylthiophene-2-carbonyl)-[1,3'-bipiperidin]-4-yl)(4-methoxyphenyl)methanone oxalate (10f)—Free base **10f** (35 mg, 84%) was obtained as a light yellow solid. ^{1}H NMR (400 MHz, $CDCl_3$) δ 7.92 (d, *J* = 8.7 Hz, 2H), 7.11 (d, *J* = 3.6 Hz, 1H), 6.94 (d, *J* = 8.9 Hz, 2H), 6.71 (d, *J* = 3.6 Hz, 1H), 4.77 – 4.61 (m, 1H), 4.52 – 4.36 (m, 1H), 3.87 (s, 3H), 3.75 – 3.55 (m, 2H), 3.30 – 3.17 (m, 1H), 3.13 – 3.04 (m, 1H), 3.00 – 2.69 (m, 4H), 2.51 (s, 3H), 2.48 – 2.31 (m, 2H), 2.19 – 2.09 (m, 1H), 1.96 – 1.69 (m, 4H), 1.61 – 1.48 (m, 1H). ^{13}C NMR (101 MHz, $CDCl_3$) δ 200.8, 163.8, 163.5, 144.0, 134.4, 130.5, 129.3, 128.9, 125.1, 113.9, 67.9, 67.8, 55.5, 52.4, 45.3, 43.3, 32.7, 29.7, 29.3, 15.3. The free base was treated with oxalic acid to afford the corresponding oxalate salt as white solid. mp: 137 °C (decomposed). Anal. ($C_{24}H_{30}N_2O_4S \cdot H_2C_2O_4 \cdot 0.5H_2O$) C, H, N.

4.2.14. (4'-Hydroxy-1'-(3-methylthiophene-2-carbonyl)-[1,3'-bi-piperidin]-4-yl) (4-methoxyphenyl)methanone oxalate (10g)—Free base **10g** (88.6 mg, 60%) was obtained as a pale solid. ^{1}H NMR (400 MHz, Chloroform-d) δ 7.93 – 7.74 (m, 2H), 7.27 – 7.15 (m, 1H), 6.94 – 6.83 (m, 2H), 6.83 – 6.71 (m, 1H), 4.76 – 4.27 (m, 1H), 4.27 – 3.93 (m, 1H), 3.80 (s, 3H), 3.71 – 3.49 (m, 2H), 3.25 – 3.07 (m, 1H), 3.07 – 2.93 (m, 1H), 2.93 – 2.57 (m, 4H), 2.46 – 2.23 (m, 2H), 2.21 (s, 3H), 2.13 – 2.00 (m, 1H), 1.88 – 1.58 (m, 4H), 1.53 – 1.34 (m, 1H). ^{13}C NMR (101 MHz, $cdcl_3$) δ 200.6, 164.5, 163.2, 137.2, 130.3, 129.8, 129.6, 128.6, 125.7, 113.6, 67.8, 67.1, 55.3, 52.0, 45.1, 43.0, 32.5, 29.4, 29.1, 14.5. The free base

was treated with oxalic acid to afford the corresponding oxalate salt as white solid. mp: 134 °C (decompose). Anal. ($C_{24}H_{30}N_2O_4S•C_2H_2O_4•1.5H_2O$) C, H, N.

4.2.15. (4-(4-Fluorobenzoyl)-3'-hydroxy-[1,4'-bipiperidin]-1'-yl)-(thiophen-2-yl)methanone oxalate (11a)—Free base **11a** (28 mg, 68%) was obtained as a colorless oil. ^{1}H NMR (400 MHz, $CDCl_3$) δ 8.03 – 7.87 (m, 2H), 7.45 (d, *J* = 5.1 Hz, 1H), 7.31 (d, *J* = 3.9 Hz, 1H), 7.14 (t, *J* = 8.6 Hz, 2H), 7.04 (dd, *J* = 5.0, 3.6 Hz, 1H), 4.89 – 4.47 (br s, 2H), 3.73 – 3.56 (br s, 1H), 3.56 – 3.43 (m, 1H), 3.31 – 3.16 (m, 1H), 3.02 – 2.91 (m, 1H), 2.91 – 2.68 (m, 4H), 2.56 – 2.41 (m, 1H), 2.35 – 2.23 (m, 1H), 1.98 – 1.82 (m, 4H), 1.82 – 1.66 (m, 1H), 1.58 – 1.46 (m, 1H). ^{13}C NMR (101 MHz, $CDCl_3$) δ 200.7, 167.0, 163.9, 136.8, 132.3, 130.8, 128.9, 128.7, 126.7, 115.7, 69.6, 65.9, 51.9, 45.2, 43.6, 29.7, 29.4, 29.2. The free base was treated with oxalic acid to afford the corresponding oxalate salt as white solid. mp: 187 °C (decomposed). Anal. ($C_{22}H_{25}FN_2O_3S•H_2C_2O_4$) C, H, N.

4.2.16. (4-(4-Fluorobenzoyl)-3'-hydroxy-[1,4'-bipiperidin]-1'-yl)(3-methylthiophen-2-yl)methanone oxalate (11b)—Free base **11b** (23 mg, 54%) was obtained as a color less oil. ^{1}H NMR (400 MHz, $CDCl_3$) δ 8.00 – 7.93 (m, 2H), 7.29 – 7.26 (m, 1H), 7.14 (t, *J* = 8.6 Hz, 2H), 6.83 (d, *J* = 4.9 Hz, 1H), 4.80 – 4.25 (m, 2H), 3.73 – 3.53 (br s, 1H), 3.50 – 3.39 (m, 1H), 3.30 – 3.17 (m, 1H), 3.00 – 2.90 (m, 1H), 2.86 – 2.69 (m, 4H), 2.52 – 2.40 (m, 1H), 2.34 – 2.27 (m, 1H), 2.26 (s, 3H), 1.96 – 1.81 (m, 4H), 1.80 – 1.67 (m, 1H), 1.56 – 1.45 (m, 1H). ^{13}C NMR (101 MHz, $CDCl_3$) δ 200.7, 167.0, 165.0, 137.5, 132.3, 130.8, 130.0, 129.8, 126.0, 115.7, 69.6, 65.9, 51.9, 45.2, 43.6, 29.7, 29.4, 29.1, 14.7. The free base was treated with oxalic acid to afford the corresponding oxalate salt as white solid. mp: 130 °C (decomposed). Anal. ($C_{23}H_{27}FN_2O_3S•H_2C_2O_4•$ $0.75H_2O$) C, H, N.

4.2.17. (3'-Hydroxy-1'-(thiophene-2-carbonyl)-[1,4'-bipiperidin]-4-yl)(4-methoxyphenyl)methanone oxalate (11c)—Free base **11c** (35 mg, 87%) was obtained as a pale solid. ^{1}H NMR (400 MHz, $CDCl_3$) δ 7.92 (d, *J* = 8.9 Hz, 2H), 7.44 (d, *J* = 4.8 Hz, 1H), 7.30 (d, *J* = 3.7 Hz, 1H), 7.04 (dd, *J* = 5.0, 3.7 Hz, 1H), 6.94 (d, *J* = 8.9 Hz, 2H), 4.82 – 4.51 (br s, 2H), 3.87 (s, 3H), 3.73 – 3.58 (br s, 1H), 3.56 – 3.44 (m, 1H), 3.30 – 3.17 (m, 1H), 3.00 – 2.90 (m, 1H), 2.90 – 2.70 (m, 4H), 2.54 – 2.42 (m, 1H), 2.35 – 2.23 (m, 1H), 1.95 – 1.83 (m, 4H), 1.81 – 1.67 (m, 1H), 1.62 – 1.47 (m, 1H). ^{13}C NMR (101 MHz, $CDCl_3$) δ 200.9, 163.9, 163.4, 136.8, 130.5, 128.9, 128.7, 126.7, 113.8, 69.6, 65.9, 55.5, 52.0, 45.3, 43.3, 29.5, 29.3, 22.0. CIMS: Calcd, 429.1843 (M+); Found, 429.1843 (M+). The purity of **11c** was greater than 95%. The free base was treated with oxalic acid to afford the corresponding oxalate salt as white solid. mp: 203 °C (decomposed). Anal. ($C_{23}H_{28}N_2O_4S•H_2C_2O_4$) C, H, N.

4.2.18. (3'-Hydroxy-1'-(5-methylthiophene-2-carbonyl)-[1,4'-bipiperidin]-4-yl)(4-methoxyphenyl)methanone oxalate (11d)—Free base **11d** (29 mg, 70%) was obtained as a colorless oil. ^{1}H NMR (400 MHz, $CDCl_3$) δ 7.93 (d, *J* = 8.8 Hz, 2H), 7.12 (d, *J* = 3.6 Hz, 1H), 6.94 (d, *J* = 8.9 Hz, 2H), 6.69 (d, *J* = 3.6 Hz, 1H), 4.83 – 4.58 (m, 2H), 3.87 (s, 3H), 3.72 – 3.58 (br s, 1H), 3.55 – 3.45 (m, 1H), 3.29 – 3.18 (m, 1H), 2.99 – 2.90 (m, 1H), 2.89 – 2.70 (m, 4H), 2.49 (s, 3H), 2.48 – 2.42 (m, 1H), 2.34 – 2.23 (m, 1H), 1.95 – 1.81 (m, 4H), 1.81 – 1.67 (m, 1H), 1.59 – 1.46 (m, 1H). ^{13}C NMR (101 MHz, $CDCl_3$) δ 200.9, 163.9, 163.5, 144.0, 134.3, 130.5, 129.5, 128.9, 125.1, 113.8, 69.7, 65.9, 55.5, 52.0, 45.3, 43.3, 29.5, 29.3, 22.0, 15.3. The free base was treated with oxalic acid to afford the corresponding oxalate salt as white solid. mp: 137 °C (decomposed). Anal. ($C_{23}H_{28}N_2O_4S•H_2C_2O_4•0.25H_2O$) C, H, N.

4.5. In vitro Biological Evaluation

Sigma Receptor Binding affinity—The compounds were dissolved in DMF, DMSO, or ethanol, and then diluted in 50 mM Tris-HCl buffer containing 150 mM NaCl and 100 mM EDTA at pH 7.4 prior to performing σ_1 and σ_2 receptor binding measurement. The detail procedures for performing the σ_1 and σ_2 receptor binding measurement have been described.[24, 32] To measure the σ_1 receptor binding affinity, guinea pig brain membrane homogenates (~300 μg protein) tissues were the receptor resource and ~5 nM [^{3}H](+)-pentazocine (34.9 Ci/mmol, Perkin-Elmer, Boston, MA). Incubation was performed in 96-well plates for 90 min at room temperature. Nonspecific binding was determined from samples temperature. Nonspecific binding was determined from samples that contained 10 μM of nonradioactive haloperidol. After 90 min, the incubation was stopped by addition of 150 μL of ice-cold wash buffer (10 mM Tris-HCl, 150 mM NaCl, pH 7.4). The harvested samples were filtered rapidly through a 96-well fiberglass filter plate (Millipore, Billerica, MA) that had been presoaked with 100 μL of 50mM Tris-HCl buffer at pH 8.0 for 60 min. Each filter was washed with 3 × 200 μL portinos of ice-cold wash buffer, and the filter was placed in a Wallac 1450 MicroBeta liquid scintillation counter (Perkin-Elmer, Boston, MA) to count the σ_2 receptor binding affinity was determined using rat liver membrane homogenates (~300 μg protein) and ~5 nM [^{3}H]DTG (58.1 Ci/mmol, Perkin-Elmer, Bostan, MA) in the presence of 1 μ of(+)- pentazocine to block σ_1 sites. The incubation time was 120 min at room temperature. Nonspecific binding was determined from samples that contained 10 μM of nonradioactive haloperidol. All other procedures were same to those describe for the σ_1 receptor binding assay above.

The concentration that inhibits 50% of the specific binding of the radioligand (IC_{50} value) was determined based on the data from competitive inhibition experiment by using nonlinear regression analysis. Competitive curves were best fit to a one-site model and gave pseudo-Hill coefficients of 0.6-1.0. K_i values were calculated using the method of Cheng and Prusoff[33] and are presented as the mean (± 1 SEM). For these calculations, we used a K_d value of 7.89 nM for [^{3}H](+)-pentazocine binding to σ_1 receptor in guinea pig brain and a K_d value of 30.7 nM for [^{3}H]DTG binding to σ_2 receptor in rat liver.

Vesicular acetylcholine transporter binding affinity—In vitro binding affinities to VAChT were conducted with human VAChT permanently expressed in PC12 cells at about 50 pmol/mg of crude extract. No significant amounts of σ_1 or σ_2 receptors were present.

The radioligand used was 5 nM (-)-[^{3}H]vesamicol, and the assay was conducted as described at final concentrations of 10^{-11} M to 10^{-5} M novel compounds.[24, 25] Unlabeled (-)-vesamicol was used as an external standard, for which K_i = 15 nM, and the mixture was allowed to equilibrate at 23 ° for 20 hours. Duplicate data were averaged and fitted by regression with a rectangular hyperbola to estimate the K_i value of the novel compound. All compounds were independently assayed at least two times.

Supplementary Material

Refer to Web version on PubMed Central for supplementary material.

Acknowledgments

Financial support for these studies was provided by the National Institutes of Health under NS061025, NS075527 MH092797, and Mcdonnell Center for Systems Neuroscience.

Abbreviation List

AD	Alzhemer's disease
ACh	acetylcholine
Anal.	Analysis
BBB	brain blood barrier
BOP-C1	bis(2-oxo-3-oxazolidinyl)phosphonic acid
C	Celsius
Calcd.	calculated
CIM.	chemical ionization mass spectrometry
DTG	1,3-ditolylguanidine
***m*-CPBA**	*meta*-chloroperoxybenzoic acid
ND	not determined
PD	Parkison's disease
PET	positron emission tomography
SPECT	single-photon emission computed tomography
VAChT	vesicular acetylcholine transporter

References and notes

1. Coyle JT, Price DL, DeLong MR. Science. 1983; 219:1184. [PubMed: 6338589]
2. Bohnen NI, Frey KA. Mol. Imag. Biol. 2007; 9:243.
3. Bohnen NI, Kaufer DI, Hendrickson R, Ivanco LS, Lopresti BJ, Constantine GM, Mathis Ch A, Davis JG, Moore RY, Dekosky ST. J. Neurol. 2006; 253:242. [PubMed: 16133720]
4. Bohnen NI, Kaufer DI, Ivanco LS, Lopresti B, Koeppe RA, Davis JG, Mathis CA, Moore RY, DeKosky ST. Arch. Neurol. 2003; 60:1745. [PubMed: 14676050]
5. DeKosky ST, Scheff SW. Ann. Neurol. 1990; 27:457. [PubMed: 2360787]
6. Marlatt MW, Webber KM, Moreira PI, Lee H-G, Casadesus G, Honda K, Zhu X, Perry G, Smith MA. Curr. Med. Chem. 2005; 12:1137. [PubMed: 15892629]
7. Siegal D, Erickson J, Varoqui H, Ang L, Kalasinsky KS, Peretti FJ, Aiken SS, Wickham DJ, Kish SJ. Synapse. 2004; 52:223. [PubMed: 15103689]
8. Terry AV Jr. Mahadik SP. J. Pharmacol. Exp. Ther. 2007; 320:961. [PubMed: 16966470]
9. Marien MR, Parsons SM, Altar CA. Proc. Natl. Acad. Sci. U. S. A. 1987; 84:876. [PubMed: 3468515]
10. Roghani A, Feldman J, Kohan SA, Shirzadi A, Gundersen CB, Brecha N, Edwards RH. Proc. Natl. Acad. Sci. U. S. A. 1994; 91:10620. [PubMed: 7938002]
11. Giboureau N, Som IM, Boucher-Arnold A, Guilloteau D, Kassiou M. Curr. Top. Med. Chem. 2010; 10:1569. [PubMed: 20583990]
12. Elwary SM, Chavan B, Schallreuter KU. J. Invest. Dermatol. 2006; 126:1879. [PubMed: 16763548]
13. de Castro BM, De Jaeger X, Martins-Silva C, Lima RD, Amaral E, Menezes C, Lima P, Neves CM, Pires RG, Gould TW, Welch I, Kushmerick C, Guatimosim C, Izquierdo I, Cammarota M, Rylett RJ, Gomez MV, Caron MG, Oppenheim RW, Prado MA, Prado VF. Mol. Cell. Biol. 2009; 29:5238. [PubMed: 19635813]
14. Prado VF, Martins-Silva C, de Castro BM, Lima RF, Barros DM, Amaral E, Ramsey AJ, Sotnikova TD, Ramirez MR, Kim HG, Rossato JI, Koenen J, Quan H, Cota VR, Moraes MF,

Gomez MV, Guatimosim C, Wetsel WC, Kushmerick C, Pereira GS, Gainetdinov RR, Izquierdo I, Caron MG, Prado MA. Neuron. 2006; 51:601. [PubMed: 16950158]

15. Anderson DC, King SC, Parsons SM. Mol. Pharmacol. 1983; 24:48. [PubMed: 6865925]
16. Carroll PT. Brain Res. 1985; 358:200. [PubMed: 4075114]
17. Michaelson DM, Burstein M. FEBS Lett. 1985; 188:389. [PubMed: 4029394]
18. Efange SM, Khare AB, Langason RB. Nucl. Med. Biol. 1995; 22:437. [PubMed: 7550019]
19. Coffeen PR, Efange SM, Haidet GC, McKnite S, Langason RB, Khare AB, Pennington J, Lurie KG. Nucl. Med. Biol. 1996; 23:923. [PubMed: 8971861]
20. Shiba K, Ogawa K, Ishiwata K, Yajima K, Mori H. Biorg. Med. Chem. 2006; 14:2620.
21. Sorger D, Scheunemann M, Vercouillie J, Großmann U, Fischer S, Hiller A, Wenzel B, Roghani A, Schliebs R, Steinbach J, Brust P, Sabri O. Nucl. Med. Biol. 2009; 36:17. [PubMed: 19181265]
22. Scheunemann M, Sorger D, Wenzel B, Heinitz K, Schliebs R, Klingner M, Sabri O, Steinbach J. Biorg. Med. Chem. 2004; 12:1459.
23. Dickey CA, Petrucelli L. Expert Opin. Ther. Tar. 2006; 10:665.
24. Efange SM, Khare AB, von Hohenberg K, Mach RH, Parsons SM, Tu Z. J. Med. Chem. 2010; 53:2825. [PubMed: 20218624]
25. Tu Z, Efange SM, Xu J, Li S, Jones LA, Parsons SM, Mach RH. J. Med. Chem. 2009; 52:1358. [PubMed: 19203271]
26. Efange SM, Khare AB, Foulon C, Akella SK, Parsons SM. J. Med. Chem. 1994; 37:2574. [PubMed: 8057300]
27. Efange SM, Mach RH, Khare A, Michelson RH, Nowak PA, Evora PH. Appl. Radiat. Isot. 1994; 45:465. [PubMed: 8186771]
28. Mach RH, Voytko ML, Ehrenkaufer RL, Nader MA, Tobin JR, Efange SM, Parsons SM, Gage HD, Smith CR, Morton TE. Synapse. 1997; 25:368. [PubMed: 9097396]
29. Alz-org. Alzheimers and Dement. 2008; 4:110.
30. Wang W, Cui J, Lu X, Padakanti PK, Xu J, Parsons SM, Luedtke RR, Rath NP, Tu Z. J. Med. Chem. 2011; 54:5362. [PubMed: 21732626]
31. Bahr BA, Parsons SM. Proc. Natl. Acad. Sci. U. S. A. 1986; 83:2267. [PubMed: 3457385]
32. Tu Z, Xu J, Jones LA, Li S, Dumstorff C, Vangveravong S, Chen DL, Wheeler KT, Welch MJ, Mach RH. J. Med. Chem. 2007; 50:3194. [PubMed: 17579383]
33. Cheng Y, Prusoff WH. Biochem. Pharmacol. 1973; 22:3099. [PubMed: 4202581]

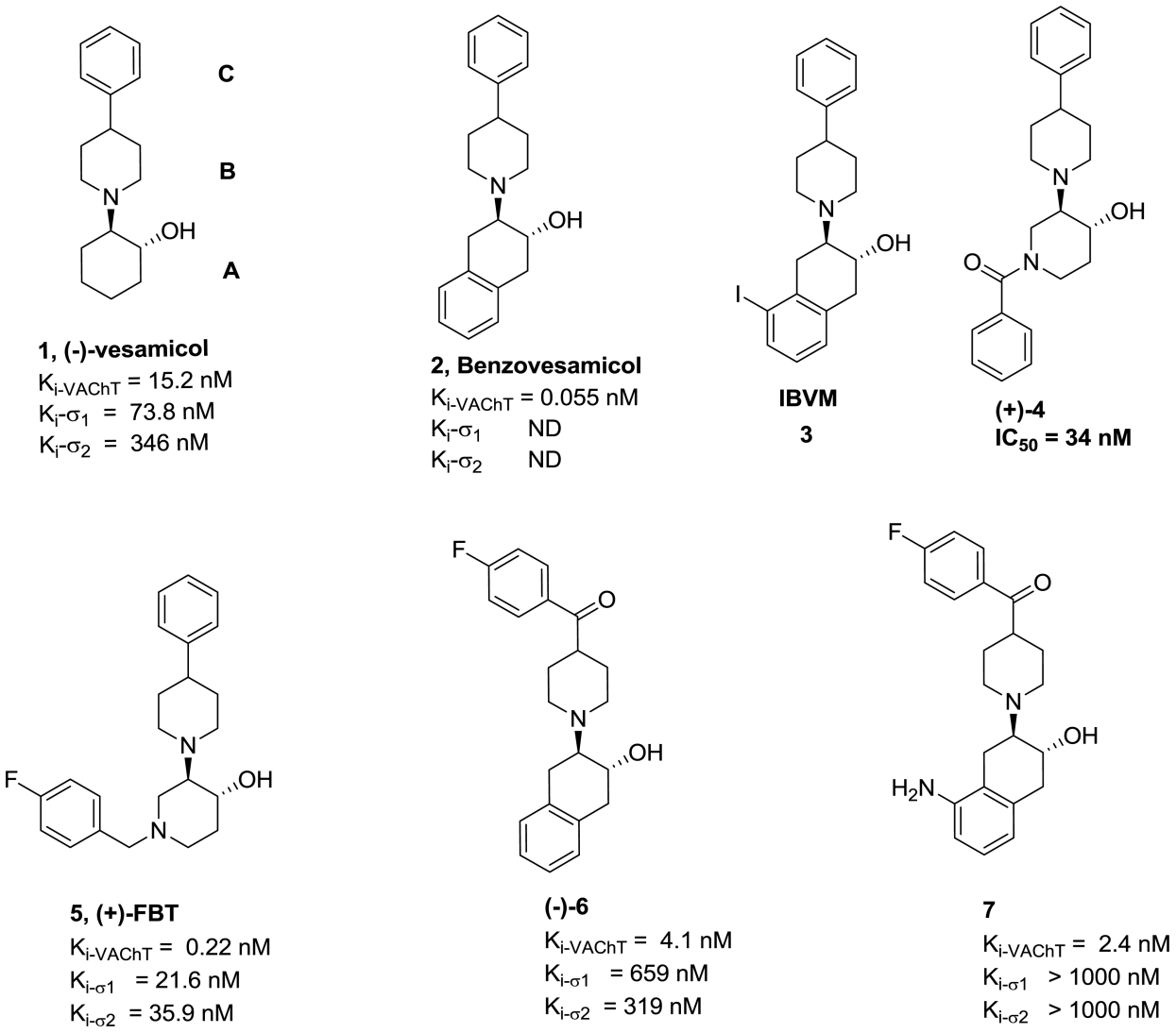

Figure 1.
Vesamicol, Benzovesamicol, Trozamicol and Related Structures

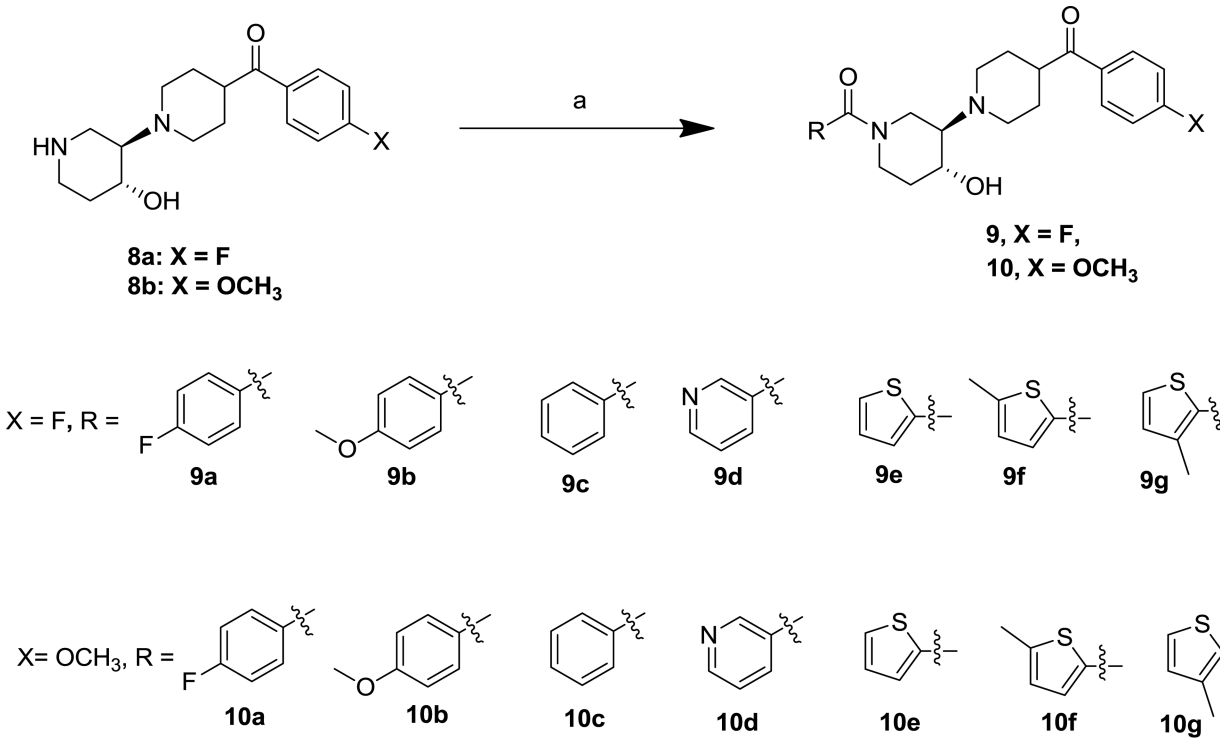

Reaction and reagent:

(a) Ar-COOH acid, BOP-Cl, $N(C_2H_5)_3$, CH_2Cl_2

Scheme 1.
Synthesis of Compounds 9a-g and 10a-g

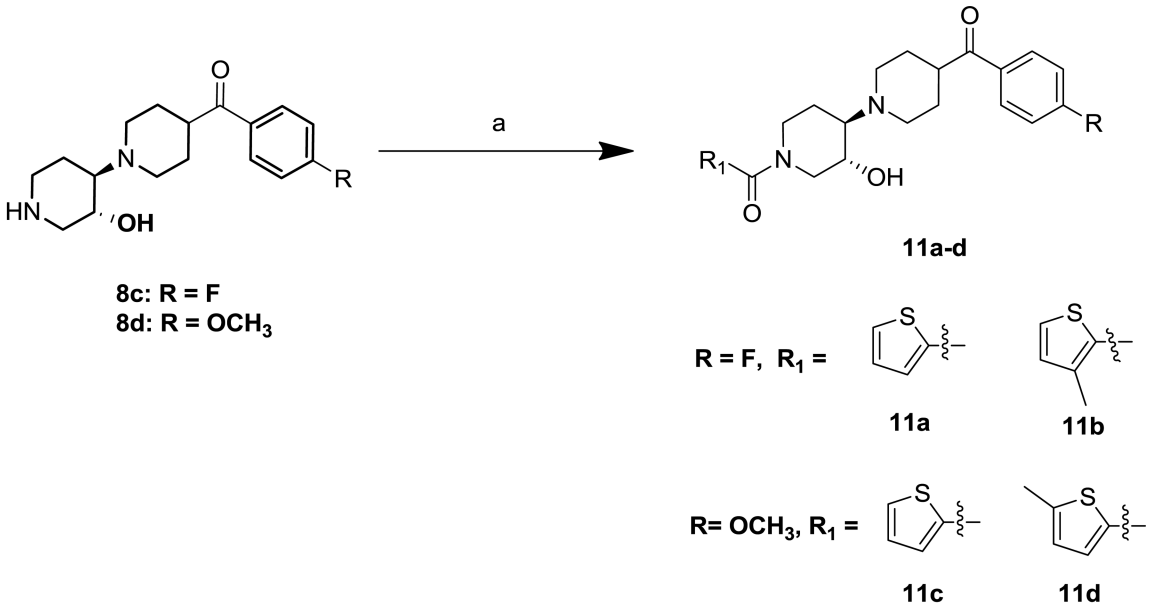

Reaction and reagent:

(a) Ar-COOH, BOP-Cl, $N(C_2H_5)_3$, CH_2Cl_2

Scheme 2.
Synthesis of Compounds 11a-d

Table 1

Affinities of new analogues for σ_1 receptor, σ_2 receptor, and VAChT[a]

Compounds	K_i (nM)			Selectivity Ratio		LogP[e]
	VAChT[d]	σ_1 [b]	σ_2 [c]	VAChT/σ_1	VAChT/σ_2	
Vesamicol	15.2 ± 1.05	73.8	346	4.86	22.8	
9a	8700 ± 1620	3119 ± 360	1375 ± 135	0.36	0.16	2.00
9b	13000 ± 1900	661 ± 72	>10000	0.05	ND	2.25
9c	62.7 ± 14.3	37900 ± 270	3950 ± 280	604	63	1.75
9d	810 ± 140	13800 ± 2600	15500 ± 2200	17.1	19.2	0.66
9e	123 ± 14.9	22500 ± 5880	4000 ± 240	183	32.9	2.07
9f	1190 ± 140	2800 ± 210	16400±1480	2.35	13.8	2.53
9g	11.4 ± 3.67	12100 ± 2400	4220 ± 200	1063	370	2.53
10a	233 ± 36.8	11900 ± 5600	2590 ± 360	51.2	11.1	1.98
10b	3020 ± 640	5260 ± 350	40400 ± 5490	1.7	7.68	2.23
10c	15.4 ± 0.94	5760 ± 480	4850 ± 650	374	315	1.73
10d	112 ± 12.9	8600 ± 380	24300 ± 1900	77	217	0.65
10e	19.0 ± 2.12	34000 ± 6120	6380 ± 1000	1787	335	2.05
10f	142 ± 16.4	39400 ± 4100	24400 ± 3600	277	172	2.51
10g	10.2 ± 0.76	15300 ± 2870	20700 ± 2670	1500	2030	2.51
11a	1300 ± 190	1660 ± 130	12300 ± 1200	1.27	1.02	1.99
11b	2020 ± 480	5770 ± 160	7830 ± 90	2.85	3.88	2.45
11c	206 ± 21.8	1334 ± 135	9709 ± 1443	6.47	47.1	1.97
11d	1350 ± 433	2340 ± 320	20500 ± 7560	1.73	15.2	2.43

[a] K_i values (mean ± SEM) were determined in at least three experiments.

[b] The σ_1 binding assay used membrane preparations of guinea pig brain.

[c] The σ_2 binding assay used homogenates of rat liver.

[d] The VAChT binding assay used expressed human VAChT.

[e] Calculated value at pH 7.4 by ACD/Labs, version 7.0 (Advanced Chemistry Development, Inc., Canada)